Intrusions of the Mediterranean Northern Current on the eastern side of the Gulf of Lion's continental shelf: characterization and generating processes

J. Gatti (1,2)*, A. Petrenko (2), C. Estournel (3), J.L. Devenon (2)

(1) Ifremer, SISMER, ZI de la Pointe du Diable, CS10070, F-29280 Plouzané, France

(2) Aix-Marseille Université, Université de Toulon, CNRS/INSU, IRD, MIO, UM110, F-13288 Marseille, France

(3) Université Paul Sabatier, CNRS, Pôle d'Océanographie Côtière de Toulouse, Laboratoire d'Aérologie, Toulouse, France

* corresponding author : julie.gatti@ifremer.fr

Abstract

The presence of Northern Current's intrusions on the continental shelf in the eastern part of the Gulf of Lion (GoL), at every season, is demonstrated with data from 12 coastal cruises (2002-2005). The intrusion flux can reach up to 0.37 Sv (10^6 m^3/s), representing 30% of the flux of the Northern Current (NC). A realistic simulation with a 3D circulation model reveals that intrusions occur about three to four times per month with a mean duration of three days and a half. Both *in situ* measurements and numerical modeling show that intrusions develop either as a separated branch of the main vein of the NC or as a part of the NC itself encroaching on the shelf. Intrusions occur at different places: at the La Ciotat canyon and Blauquières bank, between the Planier canyon and the Cassis canyon, and around the Planier canyon. Three kinds of wind events are likely to generate intrusions: the Mistral cessation, an inhomogeneous Mistral and East winds. For each case, the respective physical forcing is: upwelling relaxation, wind stress curl and Ekman drift with a shift of the current's core toward the coast. Other factors can also influence the development of intrusions such as the vertical and horizontal extents of the NC as well as its degree of mesoscale instability.

Key words: shelf-edge processes, Northern Current intrusions, GOLTS cruise stations, current data (ADCP), AVHRR images, numerical modeling, Gulf of Lion.

1. Introduction

A good knowledge of coastal circulation is necessary to define and predict the evolution of shelf ecosystems. In particular, it is of crucial importance to understand interactions between a large basin scale circulation and a shelf circulation, interactions that influence the functioning of coastal ecosystems through shelf-offshore exchanges [*Lapouyade and Durrieu de Madron*, 2001; *Durrieu de Madron et al.*, 2003; *Nencioli et al.*, 2011]. In the north western Mediterranean Sea, the Gulf of Lion (GoL, figure 1) with its wide continental shelf of about 11000 km^2 is a relevant site for such studies of interactions between coastal and offshore processes. It is bordered by the Mediterranean Northern Current (NC), the northern branch of the general cyclonic circulation in the western Mediterranean basin [*Millot and Taupier-Letage*, 2005]. The NC flows southwestward along the GoL continental slope, from the Ligurian Sea to the Catalan Sea. From a biogeochemical point of view, this oligotrophic current contrasts with shelf waters, rich in nutrients thanks to the Rhône river inputs.

Since *Millot and Wald* [1980] noticed via satellite imagery that, at the surface, the NC could reach Marseille (figure 1), some intrusions have occasionally been observed at different locations in the GoL in recent years. They occur in three main zones: the western [*Petrenko*, 2003 ; *Petrenko et al.*, 2008], central [*Estournel et al.*, 2003 ; *Petrenko*, 2003 ; *Petrenko et al.*, 2005 ; *Leredde et al.*, 2007] and eastern parts [*Albérola and Millot*, 2003 ; *Petrenko*, 2003 ; *Petrenko et al.*, 2005] of the GoL's continental shelf. Intrusions at the western part occur, whether in stratified period or not, under homogeneous Tramontane (northwest wind) conditions [*Estournel et al.*, 2003; *Petrenko et al.*, 2008]. Intrusions at the central part are generated by a double anticyclonic and cyclonic shelf circulation due to the juxtaposition of Mistral (north or northwest wind) and Tramontane winds [*Estournel et al.*, 2003; *Petrenko et al.*, 2005; *Leredde et al.*, 2007]. At the eastern entrance of the GoL, *Albérola and Millot* [2003] evidenced with current-meter data that some waters could enter on the shelf at the surface in summer and throughout the water depth in winter. They showed that these intrusions of waters influence the circulation of the bay of Cassis (figure 1), without naming them NC's intrusions. Then, *Petrenko* [2003] and *Petrenko et al.* [2005] fortuitously observed, from hull-mounted ADCP data, intrusions throughout the entire shelf's depth on the eastern part of the GoL. Up to now, intrusions on the eastern part of the shelf still remain misunderstood despite some proposed hypotheses on their generation [*Auclair et al.*, 2001; *Echevin et al.*, 2003; *Petrenko*, 2003; *Petrenko et al.*, 2005]. Hence, these eastern intrusions occurring at the entrance of the GoL are the shelf-edge processes that are detailed in this study.

Intrusions of a slope current on an adjacent shelf have also been exhibited elsewhere in the world ocean, such as the surface intrusions of the Gulf Stream by *Oey et al.* [1987] and *Gawarkiewicz et al.* [1992], and of the Kuroshio by *Chen et al.* [1996], *Tang et al.* [1999], *Wu et al.* [2005] and *Caruso et al.* [2006]. However these poleward currents are strongly influenced by the β-effect, which is not the case of the NC. Other slope currents have been observed intruding either on the northwestern shelf of the Black Sea [*Oguz and Besiktepe*, 1999; *Korotaev et al.*, 2003] or on the Papua Gulf in New Guinea [*Wolanski et al.*, 1995]; but these intrusions have not been studied in details.

The GOLTS (Gulf of Lion Time Series) project (2001-2004) has thus been planned to improve our knowledge of intrusions of a slope current on a shelf. In the framework of this project, the present paper focuses on describing and characterizing the NC's intrusions on the eastern part of the shelf, and identifying their generating processes, through both *in situ* measurements and numerical modeling. In section 2, the GOLTS experiment and the modeling study are presented before specifying the method of detection and quantification of the NC's intrusions. In section 3, both in situ and modeled results are used to qualify and quantify the intrusions. Finally, different generating processes are discussed.

2. Material and methods

The present study aims at first describing and quantifying the intrusions with the exploitation of *in situ* observations: the GOLTS data set, and second using the numerical model SYMPHONIE [*Estournel et al.*, 2009, *Marsaleix et al.*, 2008] to complete the characterization of the intrusions and analyse their generating processes. These different components are described hereafter.

2.1. The *GOLTS experiment*

In 2002-2005, the GOLTS experiment included 12 cruises (table 1) in the eastern area of the GoL's continental slope: six 5-day cruises every 6 months starting in June 2002 and six 1- to 2-day cruises of opportunity whenever the RV Tethys II was available. These cruises provided continuous currents (hull-mounted ADCP) and hydrological (thermosalinometre) data along specific transects (figure 1), as well as CTD and XBT profiles at chosen stations.

In addition to this spatial coverage of the study area, a bottom-moored ADCP has measured horizontal currents through the water column, from November 2001 to June 2006, at the edge of the continental shelf at the SOFI/GOLTS station (station 2 on figure 1 at 5.13°E and 43.07°N). Details on the hull-mounted and moored ADCP configurations are given by *Gatti et al.* [2006].

The GOLTS ship's transects have been planned as follows. The first transect (station 1 to station 6) is oriented North-South, perpendicularly to the main direction of the isobaths and thus of the NC to optimize flux calculations. It is located at the longitude of 5.13°E, longitude of the SOFI/GOLTS station. The two offshore oblique transects (station 6 to station 7 and station 4 to station 9) are also orthogonal to the isobaths near the coast to cross the NC as perpendicularly as possible. The onshore oblique transect (station 2 to station 11) allows to intercept an eventual intrusion of the NC, once on the shelf. The last transect from station 2 to station 9 is a straight segment located as closely as possible to the 200 m-deep isobath to allow a systematic detection of cross-isobath intrusions.

NOAA AVHRR images from Météo-France are used to have a synoptic coverage of SST on the entire GoL and to track the NC and its intrusions. The images analyzed in this study are those of the brightness temperature derived from the infrared channel 4 of AVHRR sensor and not absolute SST since they are used here for a qualitative description of the hydrodynamic structures. Indeed, *Taupier-Letage* [2008] has shown that such images, offering a finer resolution in both space and time, are more adequate than the noisier SST products (derived from a combination of 2 to 3 infrared channels) to track circulation features.

Wind data are provided by Météo-France at three land stations: Cape Béar, Saintes Maries and Cape Cépet (figure 1). To have synoptic wind data throughout the GoL, outputs from the ALADIN model (Météo-France) with a spatial resolution of 0.1° × 0.1° and a temporal one of 3 h are exploited.

Despite the good coverage of the zone of interest during the cruises, the measured data are not sufficient to fully describe the eastern intrusions and to understand their generating processes. Thus, modeling with the 3D circulation SYMPHONIE model has been chosen to complete the study of these shelf-edge processes.

2.2. <u>*SYMPHONIE modeling*</u>

SYMPHONIE is a 3D free surface coastal circulation model, described by *Estournel et al.* [2009] and *Marsaleix et al.* [2008, 2006]. It solves the primitive equations on a staggered C-grid using a classic finite-difference method, and applying the Boussinesq approximation and hydrostatic equilibrium hypothesis. Further details on SYMPHONIE characteristics can be found in table 2 and, together with recent applications in the GoL or the northwestern Mediterranean basin, are given by: *Reffray et al.*, [2004]; *Petrenko et al.* [2008]; *Ulses et al.* [2008a, b]; *Herrmann et al.* [2008], and *Hu et al.* [2011].

The version of SYMPHONIE used in this work is the realistic regional model developed in the framework of the MFSTEP project (Mediterranean Forecasting System Toward Environmental Predictions, http://www.bo.ingv.it/mfstep). It covers the NW Mediterranean Sea (figure 2) with a resolution of 3km×3km on the horizontal and 41 vertical levels. It is controlled by realistic forcing conditions for the first half of the year 2002. A similar model version was tested for the year 2001 by *Bouffard et al.* [2008] who compared the computed sea surface height variations with satellite altimetry.

This model is initialized and forced at its boundary by the general circulation model MOM2002 [*Pinardi et al.,* 2003]. Daily river runoffs are taken into account for the major rivers: grand Rhône, petit Rhône, Hérault, Orb, Aude and Ebre. Meteorological forcings are provided by the weather-forecast model ALADIN mentioned previously.

For the study of the influence of different meteorological conditions on intrusions' occurrence, discussed later, a specific sensitivity test is performed on east winds. Using a decreasing linear temporal "ramp", a strong east wind (maximum amplitude of 14 m/s) event has been progressively ceased in May 2002 directly in the ALADIN forcings.

The assessment of the impact of steep bathymetry requires a high-resolution grid to accurately define the canyons of the GoL's slope and to better reproduce the small-scale structures. A high-resolution nested model has been implemented in the area of the GOLTS cruises using a classic downscaling method [*Ulses et al.*, 2005; *Guizien et al.*, 2006] with one level of grid nesting. The 3 hour outputs of the large coarse-grid model (3 km × 3 km) are used to initialize and force the high-resolution model (1 km × 1 km) of the GOLTS region (5°E-6°E and 42.2°N-43.45°N; figure 2) at its open boundaries (one-way nesting). This fine-mesh simulation was used during June 2002 (period corresponding to an intrusion in the GOLTS data) to make sensitivity tests on specific bathymetric features.

2.3. *Intrusion detection and quantification*

An intrusion is defined as any vein of current flowing onshore across the 200 m-deep isobath. The GOLTS transect 2-9 (figure 1), was done during each cruise since December 2003, in order to detect intrusions, since it is parallel to the 200 m-deep isobath. The intrusions can also be detected on transects 1-2, 2-11 or 2-0 as any westward or northward current located north of the 200 m-deep isobath.

Surface hydrology cannot be used to detect intrusions of the NC. Despite the NC being well known as a warm and salty current [*Millot and Taupier-Letage*, 2005], it is hardly tracked by its variable hydrology at the entrance of the GoL. Figure 3 exhibits that the NC (which core is located between longitudes 5.4°E and 5.7°E on figure 3.a, and 5.55°E and 5.75°E on figure 3.b) can be associated either with a positive gradient in surface temperature or a negative gradient. Moreover, caution has to be taken while interpreting AVHRR images. On figure 4, warm waters are present on the shelf but are not the signature of an NC's intrusion since an eastward current is present on the entire shelf's width, from the coast to the shelf break. Alone, such hydrological data (CTD, XBT, thermosalinometre data or AVHRR images) are not sufficient to correctly detect intrusions. Hence, in this paper, current data are preferred to detect (with high reliability) the occurrence of an intrusion.

The quantification of the flux of the intrusions is performed with the hull-mounted ADCP data along the four transects described previously. Details on the flux calculation from ADCP are given by *Petrenko* [2003]. Based on all the flux obtained during GOLTS (table1), a threshold of 0.04 Sv (1 Sv = 10^6 m^3/s) is determined to define a real intrusion of the NC. It is also used as the lower limit to detect intrusions in the model outputs. The flux calculation in the model is done across the 200 m-deep isobath between stations 2 and 9 and a section extended to the coast from station 9 in order to have a complete estimation of intrusion flux (figure 2). The convention sign is: a positive flux means the current is entering onto the GoL. Any current which cross-isobathic flux is superior to 0.04 Sv is thus interpreted as a modeled intrusion. A maximum error of +/- 25% on intrusions flux has been estimated from the hull-mounted ADCP data. These maximum values are encountered in presence of inertial oscillations.

3. Description of intrusions

The GOLTS data set has been supplemented and jointly analyzed with SYMPHONIE numerical outputs to provide evidence of the existence of the NC intrusions on the eastern side of the GoL's continental shelf and to characterize them.

3.1. *Qualitative description*

Let us first describe these intrusions beginning with how the NC intrudes on the shelf. Both *in situ* measurements and numerical outputs highlight two kinds of intrusions. Intrusions develop either as a separated branch of the main vein of the NC (class 1) or as a part of the NC itself encroaching on the shelf (class 2).

The first class of intrusions can be subdivided into two sub-classes: intrusions separated from the NC core by a barotropic eastward current (class 1.a, figure 5) and those separated by a minimum of velocity (class 1.b, figure 6). The origin of barotropic eastward currents on the GoL's shelf can be various as discussed in the paper of *Gatti et al.* [2006]. Here, with our data, we determined two kinds of origin. The first origin is the generation of a barotropic eastward current after an East wind storm on the GoL [*Gatti et al.*, 2006]. The second is based on the NC mesoscale activity. The eastward current can be the northern part of an anticyclonic eddy detaching from the NC core as we can see on figure 5. From south to north, we detect the NC's core from 42.5°N to 42.9°N, the eastward current from 42.9°N to 43°N and an intrusion of the NC north of 43°N. The eastward current is present throughout all the ADCP-detected range (figure 5.b). An anticyclonic eddy with a diameter of 20 km on the inner edge of the NC can thus be inferred from these hull-mounted ADCP data. No satellite images simultaneous to this GOLTS cruise are cloudless enough to confirm the presence of this eddy, but *Flexas et al.* [2002] have previously shown with satellite images of March and April 1997 that such an eddy can develop on the inner edge of the NC. Moreover, other studies evidenced the presence of such eddies with observations from HF radars, an ADCP moorings network and

Lagrangian drifters [*André et al.*, 2009; *Allou et al.*, 2010; *Schaeffer et al.*, 2011] and with numerical outputs [*Rubio et al., 2009*; *Schaeffer et al.*, 2011]. Intrusions from the class 1.b are not separated from the NC's core by a specific feature but by a region of no current. The horizontal currents measured by the hull-mounted ADCP along a North-South transect during the GOLTS cruise of October 2002 (figure 6.a) clearly show that the intrusion is separated from the NC's core by a minimum of current around 43°N. This minimum is detected throughout all the ADCP-detected range (figure 6.b).

As regards to class 2 intrusions, a part of the NC itself can encroach on the shelf, bringing offshore waters on it. A remarkable cross-isobath intrusion was thus observed due to an extremely steep meander of the NC crossing the 200 m-deep isobath between the Planier and Cassis canyons (figure 7). This meander is well identified thanks to the superposition of an AVHRR image on the current data. Class 2 intrusions are related to the mesoscale activity of the NC and/or to the position of the NC with respect to the coast, which will be discussed in section 4.

The intrusions of both classes can spread on the entire continental shelf (figures 5 to 7), or can be very close to the coast and well isolated from the NC's core (figure 8.a). They can extend on the vertical from the surface to the bottom of the shelf (figure 6.b) with an intensity decreasing more or less quickly depending on the local stratification. These two types of intrusions can evolve from one type to the other, both in time and in space. Indeed, the intrusions observed on December 2004 changed during the five-day GOLTS cruise (figure 8). NC's meanders can generate an intrusion as a separated vein when they pass on the shelf upstream of the GoL near the Cape Sicié (figure 8.a). Then, propagating westward they can again encroach on the shelf near the Planier canyon (figure 8.b).

Shelf-slope exports have already been evidenced through the numerous canyons of the GoL slope [*Durrieu de Madron et al.*, 1999; *Dufau-Julliand et al.*, 2004; *Ulses et al.*, 2008b;

Langlais et al., 2009]. We study whether NC intrusions, in the same way, occur preferentially through canyons.

The NC intrudes on the eastern part of the GoL's shelf at different places. Class 1 intrusions usually penetrate upstream of the GoL through the La Ciotat canyon and the Blauquières bank (figure 1). A part of the NC vein can indeed detach itself from the NC near those topographic irregularities when the NC is close to the coast or when it meanders. Some of the class 1 intrusions have also been observed through the Planier canyon.

As regards to class 2 intrusions, they can occur anywhere from the La Ciotat canyon to the Planier canyon since the NC can encroach on any part of this eastern GoL's shelf.

Besides, modeling sensitivity tests with a high resolution nested simulation (1 km x 1 km) highlight that intrusions do not occur through the Cassis canyon and confirm that the promontory formed by the Blauquières bank and the La Ciotat canyon favors the separation of an intrusive branch of the NC (data not shown).

3.2. *Quantitative description*

We are first going to determine how often these intrusions occur. Such features are frequent.

During the 12 GOLTS cruises, intrusions have been observed most of the time (during 10 of the 12 cruises), except on 9 December 2003 (figure 4) and on 4 September 2004. Otherwise, they are observed to occur at every season (especially class 1 intrusions), whether the water column is stratified or not. Class 2 intrusions are more frequent in winter, when the mesoscale activity is particularly high [*Albérola et al.*, 1995; *Sammari et al.*, 1995]. Results from the bottom-moored ADCP cannot be used to study intrusions' frequency since the SOFI/GOLTS station is located most of the time downstream of the zones of intrusions.

Instead, the flux calculation with the outputs of the realistic simulation helps to detect systematically the occurrence of intrusions over the first six months of 2002 (figure 9). It reveals that, from January to June, intrusions occurred 49% of the time, about 3 or 4 times a month. They have a mean duration of 3 days and a half, ranging from one day to two weeks. The intrusion lifetime of two weeks should be considered carefully since it might be slightly overestimated due to a modeled NC closer to the coast than the measured NC.

We are now going to quantify the intrusions, estimating their flux. The measured intrusions' flux can reach up to 0.37 Sv (table 1), representing around 30% of the flux of the corresponding NC. The strongest intrusions are detected in late autumn – beginning of winter. They correspond to class 2 intrusions, encroaching of the NC on the shelf. Indeed, the maximum intensity encountered for class 1 intrusion is 0.46 m/s (on October 2002) whereas class 2 intrusions can reach up to 0.7 m/s (on December 2004). The weakest intrusions occur in summer, excepted the one in March 2004 which seems to be, from the moored ADCP data, a vanishing intrusion rather than a low flux one. The model results do not cover all the seasons, so we cannot find the same temporal variability as the measured intrusions. However, in the realistic simulation, the maximum fluxes are all obtained with class 2 intrusions as in the ADCP data. 36% of the modeled intrusions have a flux lower than 0.1 Sv and are all class 1 intrusions.

<u>4. Generating processes: discussion</u>

As evidenced previously, intrusions at the eastern part of the GoL are frequent but not permanent. This leads us to wonder which processes can break the topographic steering and induce intrusions of the NC. From the depth-averaged current vorticity equation below (corresponding to equation A.6 in appendix A which explains this formulation):

$$\beta \bar{v} - \frac{f}{H}\,\vec{\bar{u}}.\vec{\nabla}H = J\left(\chi,\frac{1}{H}\right) + J\left(\frac{g}{\rho_0}\int_{-h}^{\eta}\rho dz,\frac{h}{H}\right) + rot_z\left[\frac{\vec{\tau}^{(s)}-\vec{\tau}^{(b)}}{\rho_0 H}\right] \qquad (1)$$

as sources of relative vorticity, the GJEBAR (General Joint Effect of Baroclinicity and relief) effect (first two terms on the right hand side of the equation 1) and the wind stress curl (part of the last term of the equation 1) may play an important role in the breaking of potential vorticity conservation. Besides, it was noticed that some NC's eastern intrusions occurred during Northeast winds [*Petrenko*, 2003], others after strong Mistral [*Millot and Wald*, 1980; *Petrenko et al.*, 2005], or after Southeast winds [*Auclair et al.*, 2001]. So, the present paper focuses on the role of the wind in the generation of intrusions before studying the NC's variability as another possible cause.

<u>4.1. Wind effect</u>

Three wind regimes are predominant in the Gulf of Lion. Wind roses (figure 10) from almost five years data at the three Météo-France land stations mentioned previously (figure 1) confirm what *Millot* [1990] and *Triplet and Roche* [1986] stated: the western part of the GoL (Cape Bear) is dominated by Northwest winds (Tramontane), the central part (Saintes Maries) by North-Northwest winds (Mistral) and the eastern part (Cape Cépet) by Northwest winds (Mistral influenced by the orography) and East winds.

The GOLTS data show that around 50% of the observed intrusions occur in a Mistral context (succeeding the Mistral event or, in one case, during it) and less than 50% during an East wind event. Intrusions with the higher fluxes (on December 2003 and 2004) are encountered during the latter case. At the entrance of the GoL, the evolution of the modeled currents' flux with the wind (figure 11) confirms the conclusions issued from observations. Indeed, statistics from the 6 months simulation evidenced the occurrence of intrusions (cases of total flux superior to 0.04 Sv on figure 11) after and during moderate to strong Mistral and the development of the higher flux intrusions during East winds.

The Mistral is an upwelling favorable wind [*Millot*, 1979]. Concerning intrusions occurring after the cessation of Mistral, they thus can be interpreted as a consequence of the Cassis upwelling relaxation.

Some intrusions occurring during Mistral, and even a strong Mistral event (intensity > 10 m/s, black dots on figure 11 for wind direction > 270°), can be explained by one process: the inhomogeneity of the wind event. The Mistral should have induced export of water according to Ekman theory instead of intrusions. Analyzing in detail the modeling outputs, it appears that a Mistral favors the entrance of water at the eastern part of the GoL when it is spatially inhomogeneous. Intrusions induced by the wind stress curl effect have already been evidenced by *Estournel et al.* [2003] in the central part of the gulf. Wind stress curl is also thought to be responsible for some Kuroshio's intrusions through the Luzon strait [*Wu et al.*, 2005; *Caruso et al.*, 2006]. This effect may contribute as a source of vorticity for the depth-averaged flow (equation 1) and may generate eastern intrusions of the NC on the shelf during inhomogeneous Mistral. Indeed, during the Mistral event of March 2002, a branch of current, detached from the NC's vein, penetrates on the shelf (figure 12.a) as a consequence of the positive wind stress curl present on the eastern part of the GoL (figure 12.b).

The East wind situations inducing intrusions could be due to the action of wind through the Ekman drift and the shift of the current's core toward the coast. The wind effect on water mass transport through the Ekman drift could explain, in the case of east winds, intrusion of surface waters down to few tens of meters depth as proposed by *Oey et al.* [1987] for the Gulf

Stream's intrusions. Observed intrusions can spread over the entire depth of the GoL's shelf. In addition, a sensitivity test on east winds has been performed with SYMPHONIE and exhibits not only that there is no intrusion when the East wind event is suppressed but also that the East wind influences the NC down to 200 m depth. The NC extends until the shelf break over 200m during an East wind event (figure 13.a), whereas it does not reach the shelf break when this East wind event has been suppressed (figure 13.b). So, both the Ekman transport and the shift of the NC's core induced by the wind have to be taken into account in the generation of intrusions under East winds.

Three kinds of wind events are likely to generate intrusions: the Mistral cessation, a spatially inhomogeneous Mistral and East winds. Otherwise, intrusions cannot develop during homogeneous Mistral. Nonetheless, figure 11 illustrates that intrusions can also be detected during calm meteorological conditions (wind intensity < 5m/s), thus, other processes than wind regimes have to be analyzed.

4.2. NC's variability

The NC presents two types of variability: a seasonal variability of its intensity [*Castellón et al.*, 1990; *Albérola et al.*, 1995; *Conan and Millot*, 1995; *Petrenko*, 2003] and a variability of its spatial structure through its mesoscale activity [*Albérola et al.*, 1995; *Font et al.*, 1995; *Sammari et al.*, 1995].

From observations, the intrusions' flux has the same seasonal variability as the NC's flux. It is maximum in late autumn – beginning of winter and minimum in summer (table 1). However, in both *in situ* measurements and modeled results, high flux intrusions can develop when the NC flux is low. Intrusions exhibit a more complex variability at finer time scales than the seasonal one. That is why we believe the intrusions are rather linked to the NC's mesoscale activity than to the NC intensity. As we have seen previously, the position of the NC with respect to the coast plays a role in the process of generation of intrusions. Apart from the wind, another factor linked to the NC's core position is the NC mesoscale activity. The mesoscale activity of the NC, expressed as the development of meanders [*Crépon et al.,* 1982; *Flexas et al.*, 2002; *Petrenko, 2003*], favors shelf-offshore exchanges, and hence intrusions through the drift of the NC close to the coast. This concerns particularly class 2 intrusions (encroachings of the NC) which are a major component of the intrusions since they have the maximum fluxes. Besides, a meander of the NC can also be interpreted as a perturbation which may generate a cross-shelf transport through a propagating shelf-wave when it interacts with the shelf entrance as studied by *Echevin et al.* [2003]. A correlation of -0.91 is obtained between the modeled fluxes at the eastern part of the GoL and at the western one for extreme situations (fluxes greater than 0.12 Sv on figure 9). Moreover, considering the whole modeled dataset, a cross-correlation reveals that the fluxes entering at the eastern part of the GoL precede by around fifteen hours the fluxes exiting at the western part of the GoL. Therefore, this supports the hypothesis that an intrusion can be considered as a wave propagating from east to west on the GoL's continental shelf after interaction of a NC's meander with the shelf edge [*Echevin et al.*, 2003]. It would be necessary to track the NC's intrusions with a Lagrangian tool to further investigate their nature and determine which kind of shelf-wave they are likely to be.

Mesoscale activity thus has a key role to play in the generation of intrusions but other processes remain to be examined since intrusions also occur at period of low mesoscale instability and of calm wind.

5. Conclusions

The analysis of *in situ* measurements and satellite images during the 12 GOLTS cruises (2002-2005) evidences the occurrence, at every season, of intrusions of the NC on the eastern part of the GoL's continental shelf. Hydrological data cannot be used alone to detect systematically intrusions since the NC does not have a significant permanent hydrologic signature and often lacks contrast with shelf waters. A coupling of hydrological and current data is thus advised. Both numerical modeling and *in situ* measurements show that intrusions can develop either as a separated branch of the main vein of the NC or as a part of the NC itself encroaching on the shelf. Intrusions occur at different places: at the La Ciotat canyon and Blauquières bank, between the Planier canyon and the Cassis canyon, and around the Planier canyon. Sensitivity studies help to conclude that the Cassis canyon is not a possible way for intrusions to penetrate onto the shelf.

The observed intrusion fluxes vary with a maximum of 0.37 Sv. They can represent up to 30% of the flux of the NC. Maximum fluxes are reached in late autumn – beginning of winter due to the NC encroaching over the shelf. A realistic simulation with the SYMPHONIE model reveals that intrusions occur about three to four times per month with a mean duration of three days and a half. To improve our knowledge of their frequency, a long-time series of current from bottom to surface is necessary. Hence, we have proposed a new site for a bottom-moored ADCP: the JULIO (Judicious Location for Intrusions Observations) site (star on figure1), which has been recognized as a national observation site in the framework of the MOOSE (Mediterranean Ocean Observation multi-Sites on Environment) program. Situated on the 100 m-deep isobath, this site will allow the detection of intrusions occurring upstream the GoL through the Blauquières bank and the La Ciotat canyon as well as intrusions between the Cassis and Planier canyons. In the climate change context, *Somot et al.* [2006] have demonstrated that there would be, in the 21th century, both a decrease of the Rhone discharge and an increase of the temperature and salinity of the Mediterranean Sea. These changes could decrease dense water formation. The NC, usually considered to be directly dependent on the deep water formation, could also decrease in intensity and in mesoscale activity. Hence, a long-time series at the JULIO site will allow to follow the evolution of the NC intrusions on the shelf and to determine whether the variability of their frequency evolves.

Statistics on modeling outputs and *in situ* measurements show that three wind situations can generate intrusions of the NC on the eastern part of the shelf: the cessation of Mistral, an inhomogeneous Mistral and East winds. The Mistral can thus act on the intrusions through either the Cassis upwelling relaxation or the wind stress curl. The East winds favor eastern intrusions through the Ekman transport and NC's core drift to the coast. Other factors can also influence the development of intrusions such as the vertical and horizontal extents of the NC as well as its degree of mesoscale instability.

Other processes, likely to generate a transport across the isobaths, should be analyzed such as the Joint Effect of Baroclinicity and Relief (JEBAR, *Sarkisyan and Ivanov*, 1971; *Huthnance*, 1984; *Mertz and Wrigth*, 1992], as developed in this paper. In a numerical analysis, *Echevin et al.* [2003] have shown that the stratification of the shelf and the deepness of the NC are factors modifying the ability of the NC to penetrate on the shelf. The interaction between the density and the bathymetry should thus be analyzed in detail through a dedicated study of the JEBAR-term with numerical modeling. Finally, it appears that intrusions could propagate from east to west on the GoL's continental shelf. It would be interesting to track with a Lagrangian model the path of NC's waters once entered onto the shelf and study their impact on the coastal ecosystems.

APPENDIX A

From the Boussinesq and hydrostatic assumptions, and neglecting the advective terms (Rossby number ~ 10^{-1} within the NC), the momentum equations are given by:

$$\begin{cases} \dfrac{\partial \vec{u}}{\partial t} + f\vec{k} \times \vec{u} = -\dfrac{1}{\rho_0}\vec{\nabla} p + \dfrac{1}{\rho_0}\dfrac{\partial \vec{\tau}}{\partial z} & \text{(A.1)} \\ \dfrac{\partial p}{\partial z} = -\rho g & \text{(A.2)} \end{cases}$$

where $\vec{u} = (u, v)$ is the horizontal vector velocity, $\vec{\nabla}$ is the horizontal gradient operator, the Coriolis parameter is defined as : $f = 2\Omega\sin\Phi$ (Ω is the angular velocity vector of earth, Φ is the latitude), $\vec{k}$ is the ascendant vertical unity vector, ρ and ρ_0 are respectively the density and a reference density, p is the pressure, and $\vec{\tau} = (\tau_x, \tau_y)$ is the frictional stress.

Integrating equation (A.2) from a depth z to the free surface elevation η gives the following expression of hydrostatic pressure:

$$p = P_s + \int_z^{\eta} \rho g dz' \qquad \text{(A.3)}$$

where P_s is the ocean surface pressure.

Averaging in the vertical, equation (A.1) becomes:

$$\frac{1}{H}\int_{-h}^{\eta} \frac{\partial \vec{u}}{\partial t} dz + \frac{f}{H}\int_{-h}^{\eta} \vec{k} \times \vec{u}\, dz = -\frac{1}{H\rho_0}\int_{-h}^{\eta} \vec{\nabla} p\, dz + \frac{\left[\vec{\tau}^{(s)} - \vec{\tau}^{(b)}\right]}{H\rho_0} \qquad \text{(A.4)}$$

where h is the depth of the ocean, H represents the total depth (H=h+η), and $\vec{\tau}^{(s)}$ et $\vec{\tau}^{(b)}$ are respectively the surface and bottom frictional stresses.

Now, using the hydrostatic pressure definition (A.3) and applying the Leibniz formula, then integrating by parts, we obtain for the vertical integration of the horizontal pressure gradient:

$$\int_{-h}^{\eta} \vec{\nabla} p dz \;=\; g\vec{\nabla}\left(\int_{-h}^{\eta} \rho z dz\right) \;+\; gh\vec{\nabla}\left(\int_{-h}^{\eta} \rho dz\right) \;+\; H\vec{\nabla} P_s \qquad \text{(A.5)}$$

Cross-differentiating the equation (A.4) with the operator ($\vec{k}.\vec{\nabla}\times$) and using expression (A.5), the equation of the rate of change of the vorticity of the depth averaged flow can be written:

$$\frac{\partial \hat{\xi}}{\partial t} + \vec{k}.\vec{\nabla}\times\left(\frac{1}{H}\frac{\partial \eta}{\partial t}\left[\vec{\bar{u}} - \vec{u}_\eta\right]\right) - \frac{f}{H}\frac{\partial \eta}{\partial t} + \beta \bar{v} - \frac{f}{H}\vec{\bar{u}}.\vec{\nabla} H = J\left(\chi, \frac{1}{H}\right) + J\left(\frac{g}{\rho_0}\int_{-h}^{\eta} \rho dz, \frac{h}{H}\right) + \vec{k}.\vec{\nabla}\times\left[\frac{\vec{\tau}^{(s)} - \vec{\tau}^{(b)}}{\rho_0 H}\right]$$

$\hat{\xi}$ represents the vorticity of the depth averaged flow as referenced by *Mertz and Wright* [1992], it has the form : $\hat{\xi} = \frac{\partial}{\partial x}(\bar{v}) - \frac{\partial}{\partial y}(\bar{u})$, $\vec{\bar{u}} = (\bar{u}, \bar{v})$ where $\bar{u} = \frac{1}{H}\int_{-h}^{\eta} u dz$ and $\bar{v} = \frac{1}{H}\int_{-h}^{\eta} v dz$ are the horizontal components of the depth-averaged flow, $\vec{u}_\eta = \left(u(x,y,\eta), v(x,y,\eta)\right)$, $\beta = \frac{\partial f}{\partial y}$. The Jacobian J is defined as $J(a,b) = \frac{\partial a}{\partial x}.\frac{\partial b}{\partial y} - \frac{\partial a}{\partial y}.\frac{\partial b}{\partial x}$, and the potential energy anomaly as : $\chi = \frac{g}{\rho_0}\int_{-h}^{\eta} \rho\, z\, dz$.

The vertical component of the rotational operator ($\vec{k}.\vec{\nabla}\times$) is annotated rot_z below.

In a stationary flow, the vorticity equation of the depth averaged flow reduces to:

$$\underbrace{\beta \bar{v}}_{\text{I}} - \underbrace{\frac{f}{H}\vec{\bar{u}}.\vec{\nabla} H}_{\text{II}} = \underbrace{J\left(\chi, \frac{1}{H}\right)}_{\text{III}} + \underbrace{J\left(\frac{g}{\rho_0}\int_{-h}^{\eta} \rho dz, \frac{h}{H}\right)}_{\text{IV}} + \underbrace{rot_z\left[\frac{\vec{\tau}^{(s)} - \vec{\tau}^{(b)}}{\rho_0 H}\right]}_{\text{V}} \qquad \text{(A.6)}$$

The terms I and II come from the Coriolis term.

The balance between terms I and V corresponds to the Sverdrup theory which explains a large set of the characteristics of the global circulation at basins scale, particularly the forcing of the barotropic meridian circulation by the wind stress curl. Here, we neglect at first approximation the β term (f-plane approximation) due to the typical size of term I (10^{-12}) compared to term II (10^{-9}).

The term II of equation (A.6), neglecting the horizontal gradient of η (at maximum few cm by 100 km, i.e. ~10^{-7}) compared to the horizontal gradient of h (at minimum few tens of m by 10 km, i.e. ~10^{-3}), becomes: $-\frac{f}{H}\vec{\bar{u}}.\vec{\nabla}h$ and allow to express the behavior of a fluid with respect to isobaths as a function of sources of vorticity on the right hand side of (A.6). Without the sources terms of the right hand side of (A.6), we find that the flow is orthogonal to the gradient of h, which means it follows the isobaths.

The terms III and IV originate from the transformation of the pressure gradient term.

The term III is the classic JEBAR (Joint Effect of Baroclinicity and Relief) term used in ocean circulation at basins' scale under rigid lid approximation (e.g., *Sarkisyan and Ivanov*, 1971 ; *Huthnance*, 1984 *; Mertz and Wrigth*, 1992). It is expressed as the Jacobian of the potential energy anomaly and depth. It establishes that the combination of baroclinicity and sloping bottom topography can give rise to a driving force for the depth-averaged flow.

In the same way, the term IV is another contribution of the depth-integrated density field to the source of vorticity for the depth-averaged flow. This term exists only because we took into account the variations of the free surface elevation in this calculus.

Terms III and IV could thus be joined under the following general designation: GJEBAR which stands for "General Joint Effect of Baroclinicity and Relief". *Dippner* [1998] also obtained these two terms.

Finally, the term V represents the contribution of the wind stress curl and of the bottom torque to the source of vorticity.

ACKNOWLEDGMENTS

The GOLTS project was supported by the French PATOM (Programme Atmosphère et Océan à multi-échelles) and PNEC (Programme National d'Environnement Côtier) programs. We thank Météo-France for permission to use the output of the meteorological model ALADIN and for providing AVHRR satellite images. We are grateful to the captains and the crews of the R/V Tethys II, to Gilles Rougier and Jean-Luc Fuda for their help. We also thank the DT/INSU and Pierre-Michel Theveny for the ADCP data treatment.

The GOLTS data for this paper are available via the SISMER database (the French NODC, http://www.ifremer.fr/sismer/UK/donnees_UK.htm) for hydrologic data and via the SAVED database (CNRS-DT/INSU, http://saved.dt.insu.cnrs.fr/) for ADCP data. The AVHRR satellite images and the wind station data can be purchased from Météo-France (https://donneespubliques.meteofrance.fr/). The SYMPHONIE ocean model can be downloaded from the SIROCCO system team (http://sirocco.omp.obs-mip.fr/outils/Symphonie/Sources/SymphonieSource.htm). The numerical outputs are archived in the MIO and can be asked to one of the co-authors.

REFERENCES

Albérola, C., and C. Millot (2003), Circulation in the French mediterranean coastal zone near Marseilles: the influence of wind and the Northern Current, *Continental Shelf Research* 23, 587-610.

Albérola, C., C. Millot, and J. Font (1995), On the seasonal and mesoscale variabilities of the Northern Current during the PRIMO-0 experiment in the western Mediterranean Sea, *Oceanologica Acta* 18 (2), 163-192.

Allou, A., P. Forget, and J.-L. Devenon (2010), Submesoscale vortex structures at the eastern entrance of the Gulf of Lions in the Northwestern Mediterranean Sea, *Continental Shelf Research*, 30 (7), 724-732.

André, G., P. Garreau, and P. Fraunié (2009), Mesoscale slope current variability in the Gulf of Lions. Interpretation of in situ measurements using a three dimensional model, *Continental Shelf Research*, 29 (2), 407-423.

Asselin, R. (1972), Frequency filters for time integrations, *Monthly Weather Review* 100, 487-490.

Auclair, F., P. Marsaleix, and C. Estournel (2001), The penetration of the Northern Current over the Gulf of Lions (Mediterranean) as a downscaling problem, *Oceanologica Acta* 24, 529-544.

Beckers, J.M. (1995), La Méditerranée occidentale: de la modélisation mathématique à la simulation numérique, *PhD Thesis*, Université de Liège, Belgique, *Collection des publications de la Faculté des Sciences Appliquées*, n°136, 342pp.

Blumberg, A.F., and G.L. Mellor (1987), A description of a three-dimensional coastal ocean circulation model, in *Three-Dimensional coastal ocean models*, edited by Norman S. Heaps, pp. 1-16.

Bouffard, J., S. Vignudelli, M. Herrmann, F. Lyard, P. Marsaleix, Y. Ménard, and P. Cipollini (2008), Comparison of ocean dynamics with a regional circulation model and improved altimetry in the North-western Mediterranean, *Terrestrial, Atmospheric and Oceanic Sciences*, 19, No 1-2, 117-133, doi: 10.3319/TAO.2008.19.1-2.117(SA).

Caruso, M., G. Gawarkiewicz, and R. Beardsley (2006), Interannual variability of the Kuroshio intrusion in the South China Sea, *Journal of Oceanography* 62, 559-575.

Castellón, A., J. Font, and E. García (1990), The Liguro-Provençal-Catalan current (NW Mediterranean) observed by Doppler profiling in the Balearic Sea, *Scientia Marina* 54 (3), 269-276.

Chen, H.-T., X.-H. Yan, P.-T. Shaw and Q. Zheng (1996), A numerical simulation of wind stress and topographic effects on the Kuroshio Current path near Taiwan, *Journal of Physical Oceanography*, 26, 1769-1802.

Conan, P., and C. Millot (1995), Variability of the northern current off Marseilles, western Mediterranean Sea, from February to June 1992, *Oceanologica Acta*, 18 (2), 193-205.

Crépon, M., L. Wald, and L. M. Monget (1982), Low-frequency waves in the Ligurian Sea during december 1977, *Journal of Geophysical Research*, 87 (C1), 595-600.

Dippner, J. (1998), Vorticity analysis of transient shallow water eddy fields at the river plume front of the River Elbe in German Bight, *Journal of Marine Systems*, 14, 117-133.

Dufau-Julliand, C., P. Marsaleix, A. Petrenko, and I. Dekeyser (2004), Three-dimensional modeling of the Gulf of Lion's hydrodynamics (northwest Mediterranean) during January 1999 (MOOGLI3 Experiment) and late winter 1999: Western Mediterranean Intermediate Water's (WIW's) formation and its cascading over the shelf break, *Journal of Geophysical Research*, 109, C11002, doi:10.1029/2003JC002019.

Durrieu de Madron, X., O. Radakovitch, S. Heussner, M. D. Loÿe-Pilot, and A. Monaco (1999), Role of the climatological and current variability on shelf-slope exchanges of particulate matter: Evidence from the Rhône continental margin (NW Mediterranean), *Deep Sea Research I* 46, 1513-1538.

Durrieu de Madron, X., L. Denis, F. Diaz, N. Carcia, C. Guieu, C. Grenz, M. D. Loÿe-Pilot, W. Ludwig, T. Moutin, P. Raimbault, and C. Ridame (2003), Nutrients and carbone budgets for the Gulf of Lion during the Moogli cruises, *Oceanologica Acta* 26, 421-433.

Echevin, V., M. Crépon, and L. Mortier (2003), Interaction of a coastal current with a gulf : application to the shelf circulation of the Gulf of Lions in the Mediterranean Sea, *Journal of Physical Oceanography* 33, 188-206.

Estournel, C., V. Kondrachoff, P. Marsaleix, and R. Vehil (1997), The plume of the Rhone: numerical simulation and remote sensing, *Continental Shelf Research* 17, 899-924.

Estournel C., P. Broche, P. Marsaleix, J.L. Devenon, F. Auclair, and R. Vehil (2001), The Rhone river plume in unsteady conditions: numerical and experimental results, *Estuarine, Coastal and Shelf Science*. 53, 25-38. doi:10.1006/ecss.2000.0685

Estournel, C., X. Durrieu de Madron, P. Marsaleix, F. Auclair, C. Julliand, and R. Vehil (2003), Observation and modeling of the winter coastal oceanic circulation in the Gulf of Lion under wind conditions influenced by the continental orography (FETCH experiment). *Journal of Geophysical Research,* 108 (C3), 8059, doi:10.1029/2001JC000825.

Estournel, C., F. Auclair, M. Lux, C. Nguyen, and P. Marsaleix (2009), Scale oriented embedded modeling of the North-Western Mediterranean in the frame of MFSTEP, *Ocean Science*, 5, 73-90.

Flexas, M.M., X. Durrieu de Madron, M.A. Garcia, M. Canals, and P. Arnau, (2002), Flow variability in the Gulf of Lions during the MATER HFF experiment (March-May 1997), *Journal of Marine Systems* 33-34, 197-214.

Font, J., E. García-Ladona, and E.G. Gorriz (1995), The seasonality of the mesoscale motion in the Northern Current of the western Mediterranean: several years of evidence, *Oceanologica Acta* 18, 207-219.

Gaspar, P., Y. Gregoris, and J.-M. Lefevre (1990), A simple eddy kinetic energy model for simulations of the oceanic vertical mixing : tests at station PaPa and long-term upper ocean study site, *Journal of Geophysical Research* 95 (C9), 16179-16193.

Gatti, J., A. Petrenko, J.L. Devenon, Y. Leredde, and C. Ulses (2006), The Rhone river dilution zone present in the northeastern shelf of the Gulf of Lion in December 2003, *Continental Shelf Research* 26, 1794-1805.

Gawarkiewicz, G., T. Church, G. Luther, T. Ferdelman, and M. Caruso (1992), Large-scale penetration of Gulf Stream water onto the continental shelf north of Cape Hatteras, *Geophysical Research Letters* 19, 373-376.

Geernaert, G. L. (1990), Bulk parameterizations for the wind stress and heat fluxes, in *Surface waves and fluxes*, edited by G. L. Geernaert, and W. J. Plant, I, pp. 91–192.

Guizien, K., T. Brochier, J.-C. Duchêne, B.-S. Koh, and P. Marsaleix (2006), Dispersal of owenia fusiformis larvae by wind-driven currents: Turbulence, swimming behaviour and mortality in a three-dimensional stochastic model, *Mar. Ecol. Prog. Ser*., 311, 47-66.

Herrmann M., C. Estournel, M. Déqué, P. Marsaleix, F. Sevault, and S. Somot (2008), Dense water formation in the Gulf of Lions shelf: Impact of atmospheric interannual variability and climate change, *Continental shelf research*, 28, 2092-2112 doi:10.1016/j.csr.2008.03.003

Hu, Z.Y., A.A. Petrenko, A.M. Doglioli, and I. Dekeyser, (2011), Numerical study of eddy generation in the western part of the Gulf of Lion, *Journal of Geophysical Research* 116, C12030, doi:10.1029/2011JC007074.

Huthnance, J.M. (1984), Slope currents and "JEBAR", *Journal of Physical Oceanography* 14, 795-810.

Korotaev, G., T. Oguz, A. Nikiforov, and C. Koblinsky (2003), Seasonal, interannual, and mesoscale variability of the Black Sea upper layer circulation derived from altimeter data, *Journal of Geophysical Research* 108 (C4), doi:10.1029/2002JC001508.

Langlais, C., B. Barnier, J.-M. Molines, P. Fraunié, D. Jacob, and S. Kotlarski (2009), Evaluation of a dynamically downscaled atmospheric reanalyse in the prospect of forcing long term simulations of the ocean circulation in the Gulf of lions, *Ocean Modelling*, 30, 270-286.

Lapouyade, A., and X. Durrieu de Madron (2001), Seasonal variability of the advective transport of particulate matter and organic carbon in the Gulf of Lion (NW Mediterranean), *Oceanologica Acta* 24, 295-312.

Leredde, Y., C. Denamiel, E. Brambilla, C. Lauer-Leredde, F. Bouchette, and P. Marsaleix (2007), Hydrodynamics in the Gulf of Aigues-Mortes, NW Mediterranean Sea : *in situ* and modelling data, *Continental Shelf Research* 27, 2389-2406.

Marsaleix, P., F. Auclair, and C. Estournel (2006), Considerations on Open Boundary Conditions for Regional and Coastal ocean Models, *Journal of Atmospheric and Oceanic Technology* 23, 1604-1613.

Marsaleix, P., F. Auclair, J. W. Floor, M. J. Herrmann, C. Estournel, I. Pairaud, and C. Ulses (2008), Energy conservation issues in sigma-coordinate free-surface ocean models, *Ocean Modelling* 20, 61-89.

Mertz, G. and D.G. Wright (1992), Interpretations of the JEBAR term, *Journal of Physical Oceanography*, 22, 301-305.

Millot, C. (1979), Wind induced upwellings in the Gulf of Lions, *Oceanologica Acta,* 2, 261-174.

Millot, C. (1990), The Gulf of Lion's hydrodynamics, *Continental Shelf Research* 10, 885-894.

Millot, C., and I. Taupier-Letage (2005), Circulation in the Mediterranean Sea, in *The Mediterranean Sea: The Handbook of Environmental Chemistry*, volume 5, part K, edited by A. Saliot, pp. 29-66.

Millot, C., and L. Wald (1980), The effect of Mistral wind on the Ligurian current near Provence, *Oceanologica Acta,* 3, 399-402.

Nencioli, F., F. d'Ovidio, A. M. Doglioli, and A. A. Petrenko (2011), Surface coastal circulation patterns by in-situ detection of Lagrangian coherent structures, *Geophysical Research Letters* 38, L17604, doi:10.1029/2011GL048815.

Oey, L.Y., L. Atkinson, and J. Blanton (1987), Shoreward intrusion of upper Gulf Stream water onto the U.S. southeastern continental shelf, *Journal of Physical Oceanography,* 17, 2318-2333.

Oguz, T., and S. Besiktepe (1999), Observations on the Rim Current structure, CIW formation and transport in the western Black Sea, *Deep-Sea Research I,* 46, 1733-1753.

Petrenko, A. (2003), Variability of circulation features in the Gulf of Lion NW Mediterranean Sea. Importance of inertial currents, *Oceanologica Acta,* 26, 323-338.

Petrenko, A.A., Y. Leredde, and P. Marsaleix (2005), Circulation in a stratified and wind-forced Gulf of Lions, NW Mediterranean Sea: in situ and modeling data, *Continental Shelf Research* 25, 7-27.

Petrenko, A., C. Dufau, and C. Estournel (2008), Barotropic eastward currents in the western Gulf of Lion, north-western Mediterranean Sea, during stratified conditions, *Journal of Marine Systems*, 74, 406-428.

Pinardi, N., I. Allen, E. Demirov, P. De Mey, G. Korres, A. Lascaratos, P.Y. Le Traon, C. Maillard, G. Manzella, and C. Tziavos (2003), The Mediterranean ocean forecasting system: first phase of implementation (1998-2001), *Annales Geophysicae*, 21, 3-20.

Reffray G., P. Fraunié, and P. Marsaleix (2004), Secondary flows induced by wind forcing in the Rhône region of freshwater influence, *Ocean Dynamics*, 54, 179-196.

Rubio, A., B. Barnier, G. Jordà, M. Espino, and P. Marsaleix (2009), Origin and dynamics of mesoscale eddies in the Catalan Sea (NW Mediterranean) : Insight from a numerical model study, *Journal of Geophysical Research*, 114, C06009, doi:10.1029/2007JC004245.

Sammari, S., C. Millot, and L. Prieur (1995), Aspects of the seasonal and mesoscale variabilities of the Northern Current in the western Mediterranean Sea inferred from PROLOG-2 and PROS-6 experiments, *Deep-Sea Research I,* 42 (6), 893-917.

Sarkisyan, A.S., and V.F. Ivanov (1971), Joint effect of baroclinicity and bottom relief as an important factor in the dynamics of sea currents, *Izv. Akad. Nauk SSSR, Fiz. Atmos. Okeana* 7, 173-188.

Schaeffer, A., A. Molcard, P. Forget, P. Fraunié, and P. Garreau (2011), Generation mechanisms for mesoscale eddies in the Gulf of lions: radar observation and modeling, *Ocean Dynamics*, 61, 1587-1609.

Somot, S., F. Sevault, and M. Déqué (2006), Transient climate change scenario simulation of the Mediterranean Sea for the twenty-first century using high-resolution ocean circulation model, *Climate Dynamics*, 27, 851-879.

Tang, T.Y., Y. Hsueh, Y.J. Yang, and J.C. Ma (1999), Continental slope flow northeast of Taiwan, *Journal of Physical Oceanography*, 29, 1353-1362.

Taupier-Letage, I. (2008), On the Use of Thermal Images for Circulation Studies: Applications to the Eastern Mediterranean Basin, in *Remote Sensing of the European Sea*, edited by V. Barale and M. Gade, Springer Verlag, pp.153-164.

Triplet, J.P., and G. Roche (1986), Météorologie Générale, Météo-France, 3° edition.

Ulses, C., C. Grenz, P. Marsaleix, E. Schaaff, C. Estournel, S. Meulé, and C. Pinazo (2005), Circulation in a semi enclosed bay under the influence of strong fresh water input, *Journal of Marine Systems*, 56, 113-132.

Ulses C., C. Estournel, J. Bonnin, X. Durrieu de Madron, and P. Marsaleix (2008a). Impact of storms and dense water cascading on shelf-slope exchanges in the Gulf of Lion (NW Mediterranean). *Journal of Geophysical Research,* 113, C02010, doi:10.1029/2006JC003795.

Ulses, C., C. Estournel, P. Puig, X. Durrieu de Madron, and P. Marsaleix (2008b), Dense shelf water cascading in the northwestern Mediterranean during the cold winter 2005 : quantification of the export through the gulf of Lion and the Catalan margin, *Geophysical Research Letter*, 35, L07610, doi:10.1029/2008GL033257.

Wolanski, E., A. Norro, and B. King (1995), Water circulation in the Gulf of Papua, *Continental Shelf Research*, 15, 185-212.

Wu, C.R., T.Y. Tang, and S.F. Lin (2005), Intra-seasonal variation in the velocity field of the northeastern South China Sea. *Continental Shelf Research*, 25, 2075-2083.

FIGURES

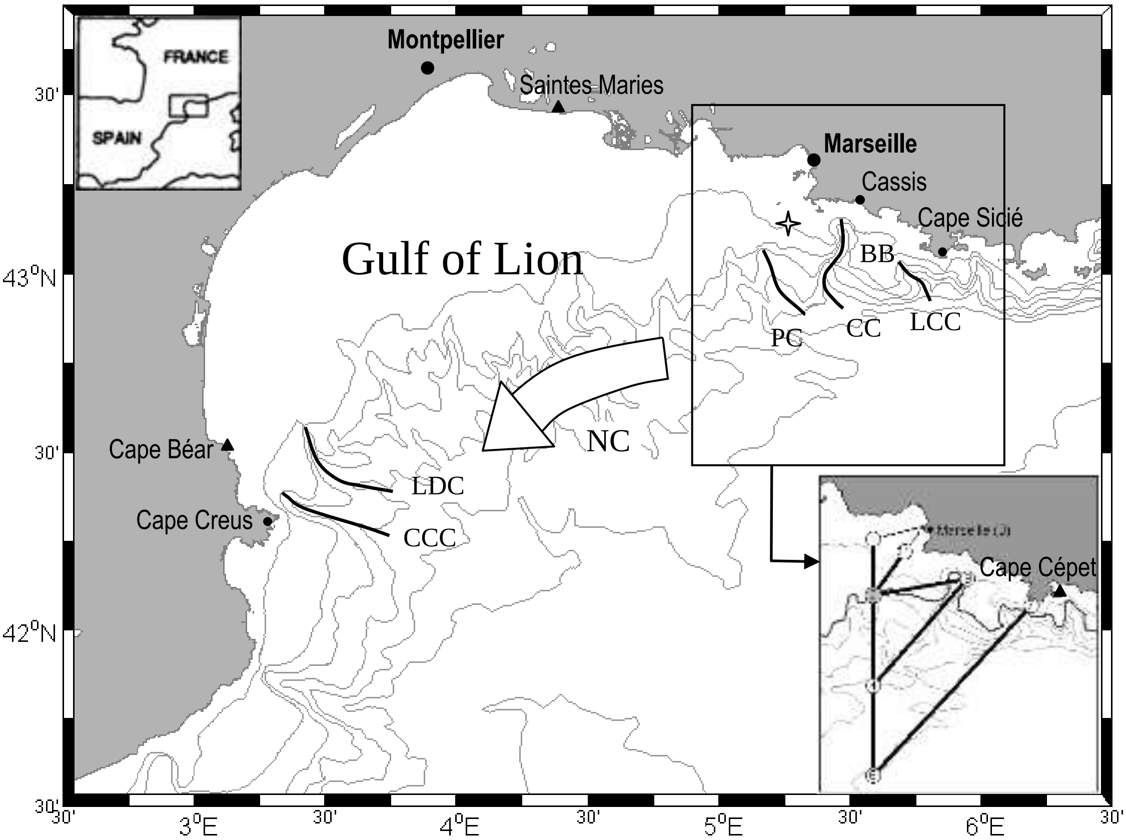

Figure 1: Gulf of Lion’s bathymetry with from east to west : the La Ciotat canyon (LCC), the Blauquières bank (BB), the Cassis canyon (CC), the Planier canyon (PC), the Lacaze-Duthiers canyon (LDC) and the Cape Creus canyon (CCC), with the branch of the NC (white arrow) flowing westward along the shelf break, the position of the JULIO mooring (star) and in the bottom right corner a zoom on the eastern part of the Gulf of Lion with the GOLTS cruise transects. Isobaths at 100, 200, 500, 1000, 1500, 2000, 2500 m are drawn.

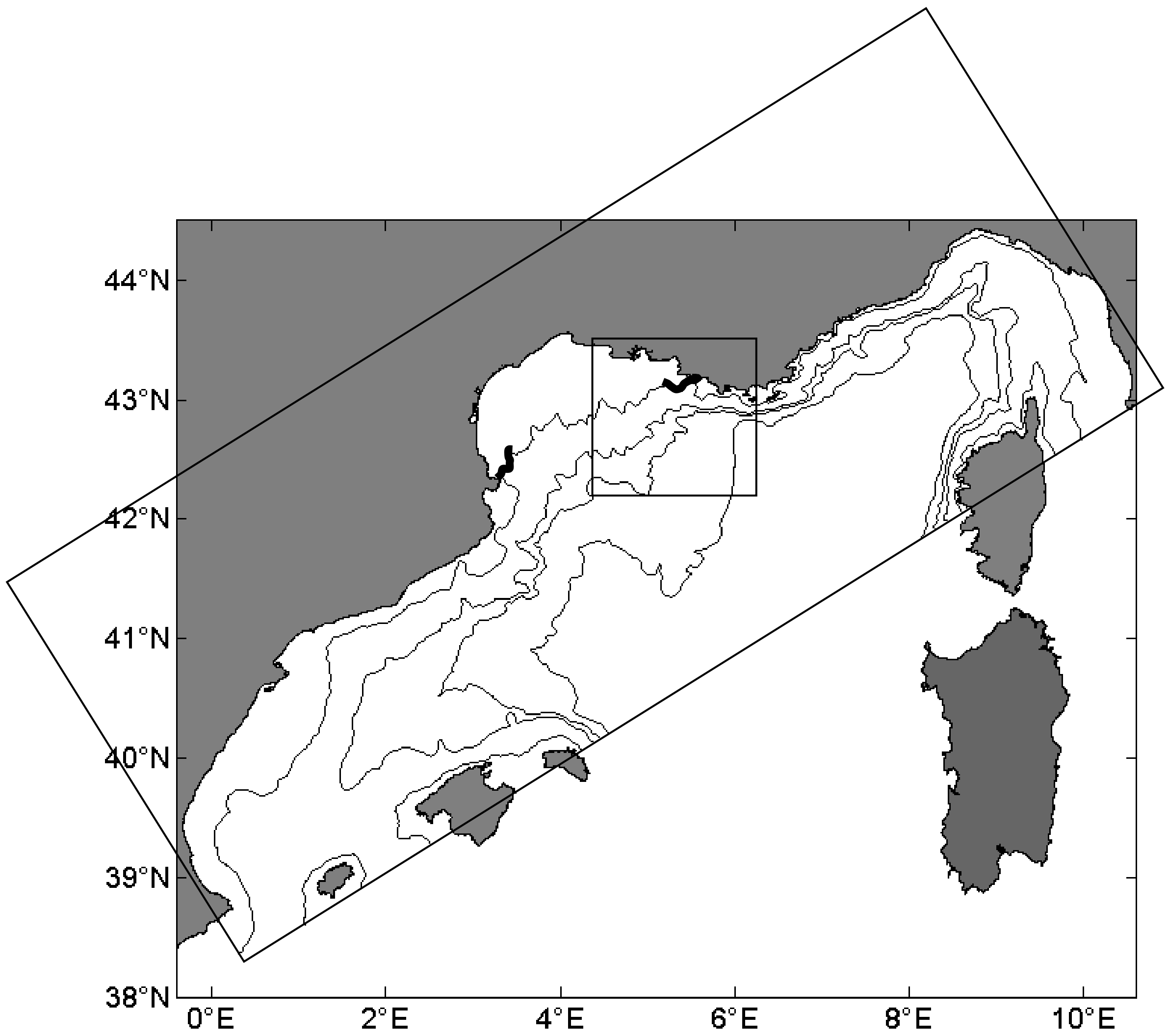

Figure 2: 3 km × 3 km modeling domain in the north-western Mediterranean (big rectangle) and 1 km × 1 km nested domain (small square). The bold lines are parts of the 200 m-deep isobath through which the current fluxes are calculated. Isobaths at 200, 1500, 2000, 2500 m are drawn in the modeling area.

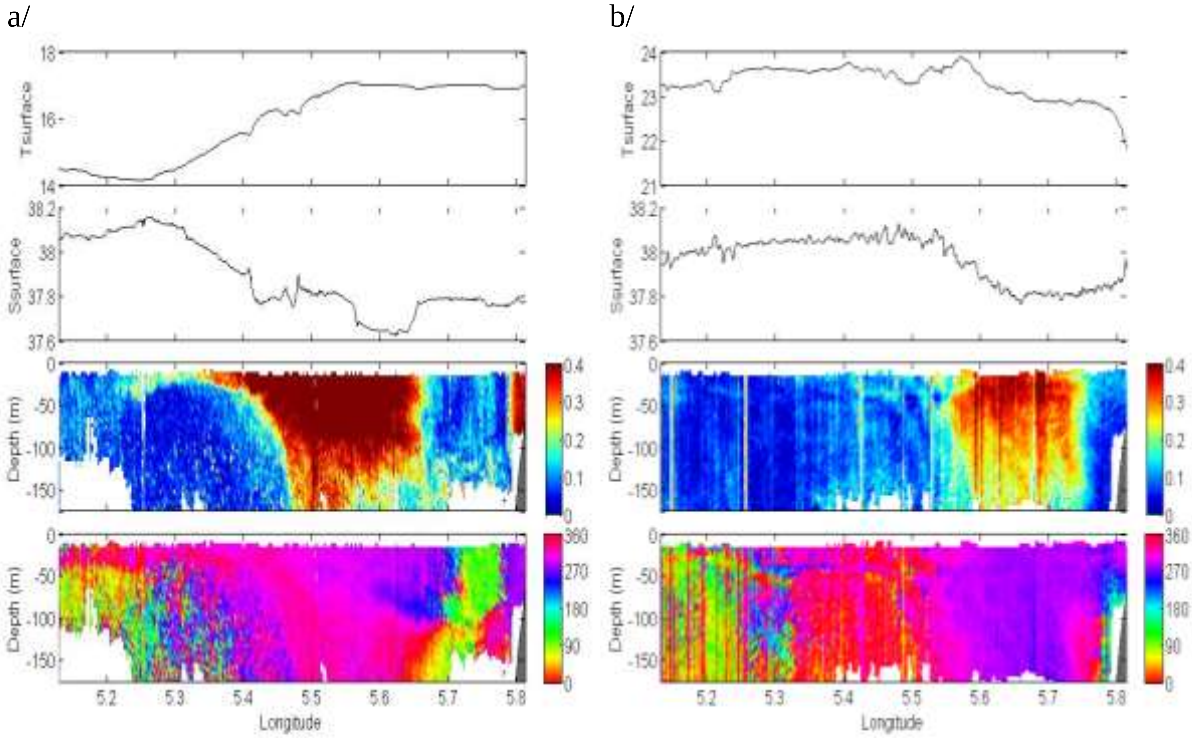

Figure 3: (from top to bottom) surface temperature, surface salinity, and vertical sections of current intensity (m/s) and current direction (°) along the transect 6-7 (figure1) during two different GOLTS cruises: a/ on December 2002, b/ on June 2003. Isotach at 0.20 m/s is drawn in white on the current intensity plot to localize the NC core.

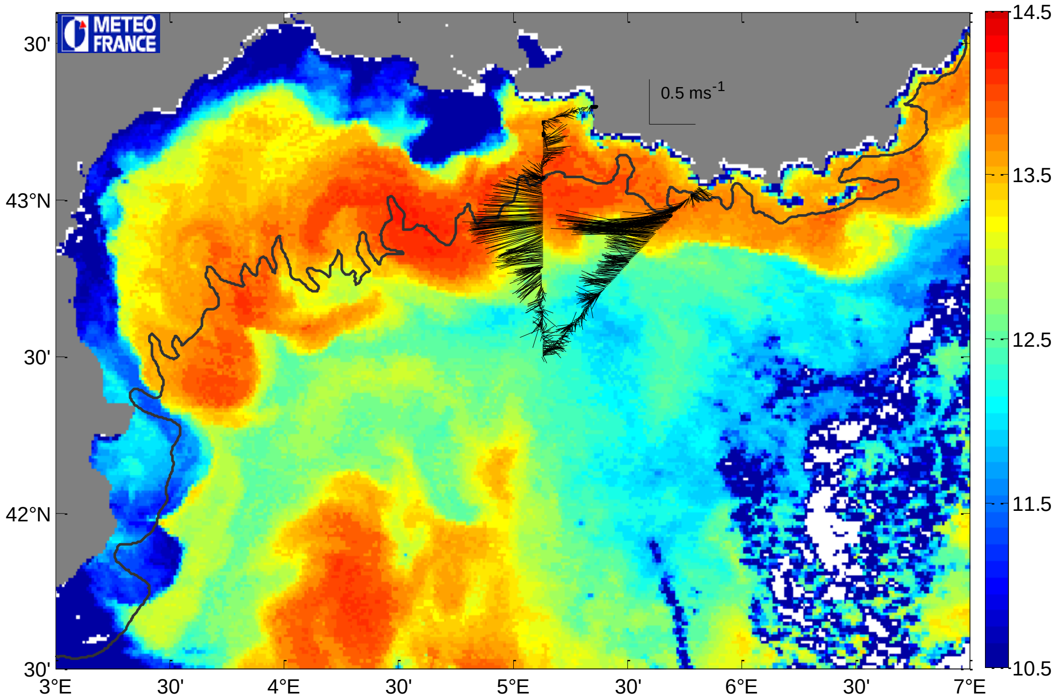

Figure 4 : AVHRR image of brightness sea surface temperature (°C) on 9 December 2003 (2h43 AM), clouds are in white. ADCP currents measured at 24 m from 4h35 AM on 9 December 2003 off Marseille are shown in black sticks. Isobaths at 200 m (black line) is drawn.

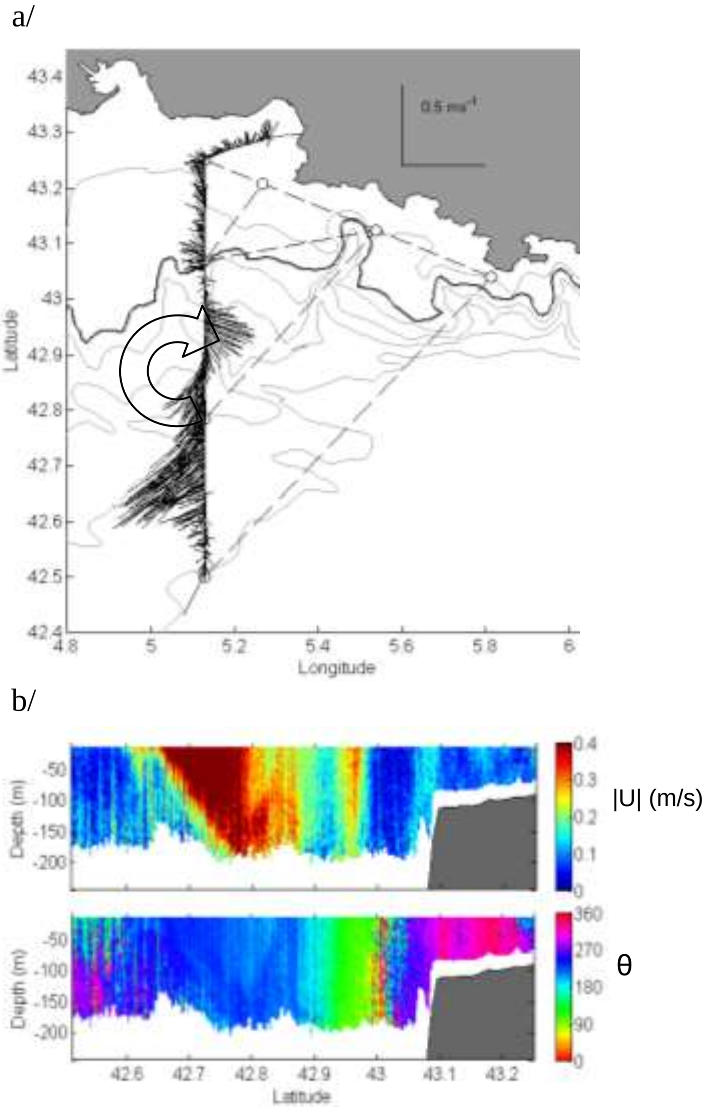

Figure 5 : a/ ADCP currents measured at 48 m on March 2003. Isobaths at 100, 200, 500, 1000, 1500 and 2000 m are drawn, b/ vertical sections of the ADCP currents intensity (m/s) and direction (°) measured along the transect 1 to 6 (figure 1).

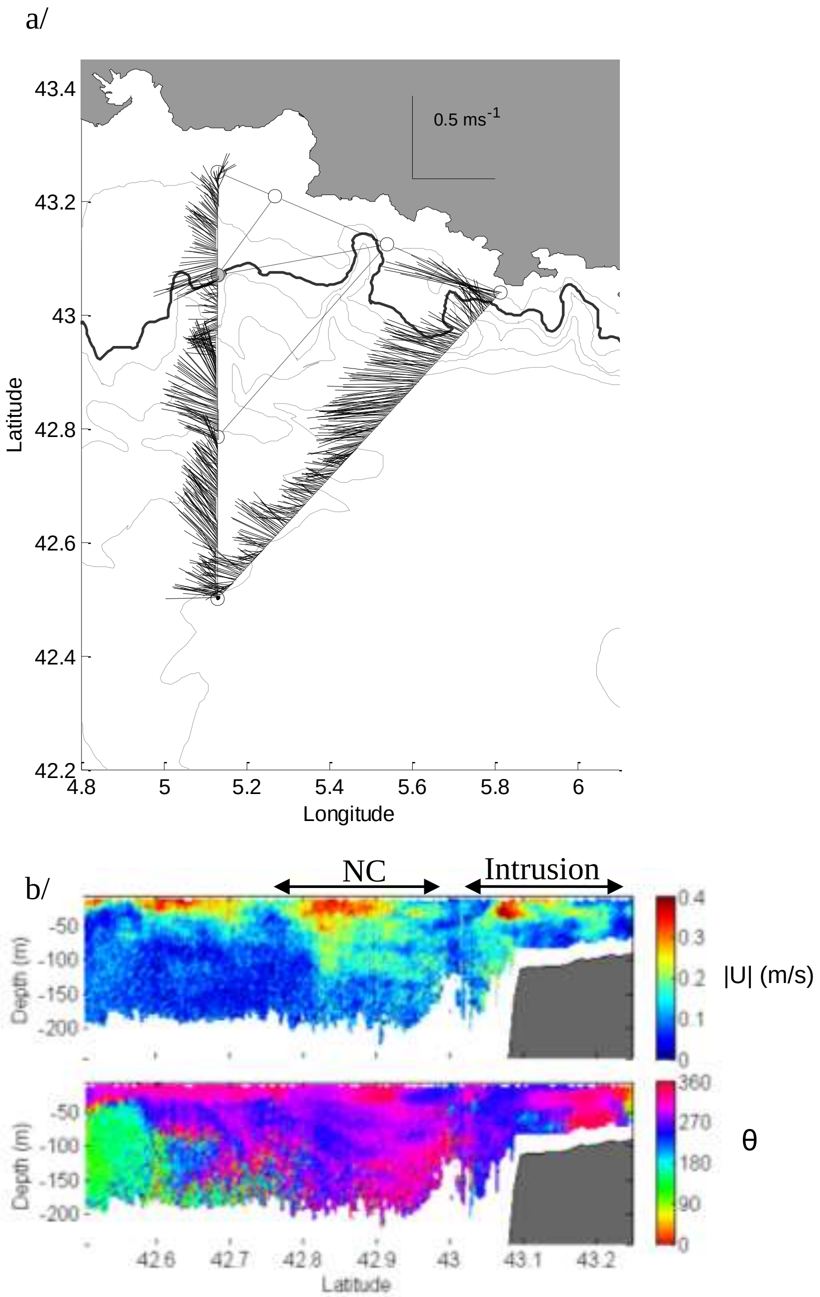

Figure 6 : a/ ADCP currents measured at 24 m on October 2002. Isobaths at 100, 200 (bold), 500, 1000, 1500 and 2000 m are drawn. b/ vertical sections of the ADCP currents intensity (m/s) and direction (°) measured along the transect 1 to 6.

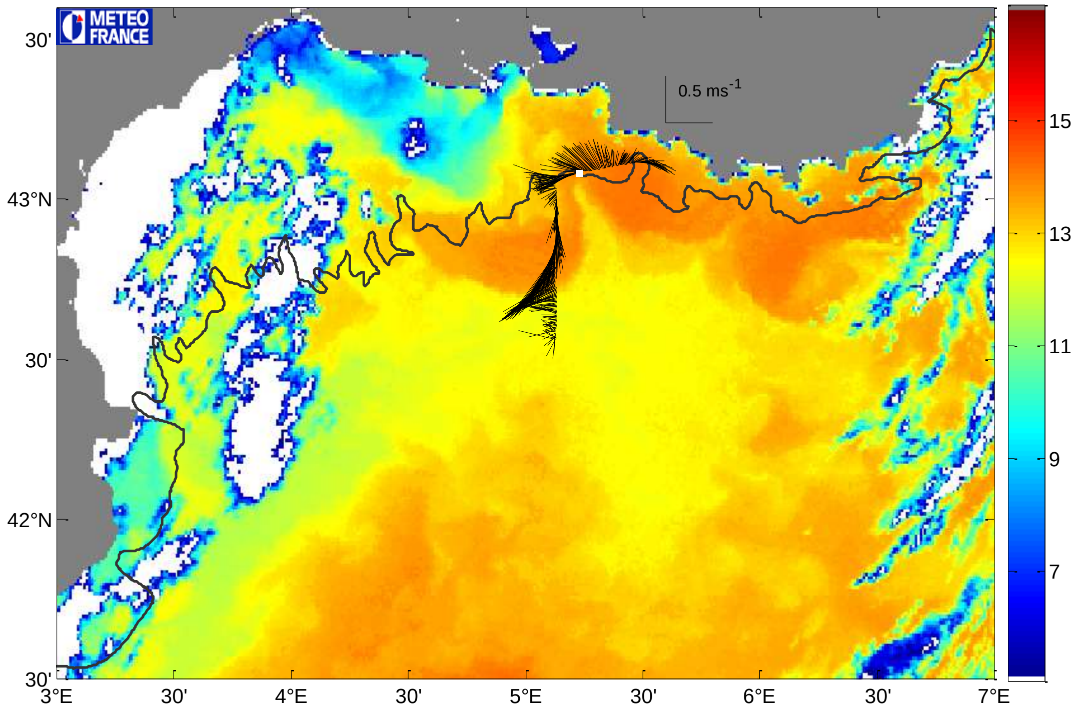

Figure 7: AVHRR image of brightness sea surface temperature (°C) on 12 December 2003 (2h09 AM), clouds are in white. ADCP currents measured at 24 m are shown in black sticks. The white square indicates the research vessel position when the AVHRR image was measured. Isobaths at 200 m (black line) is drawn.

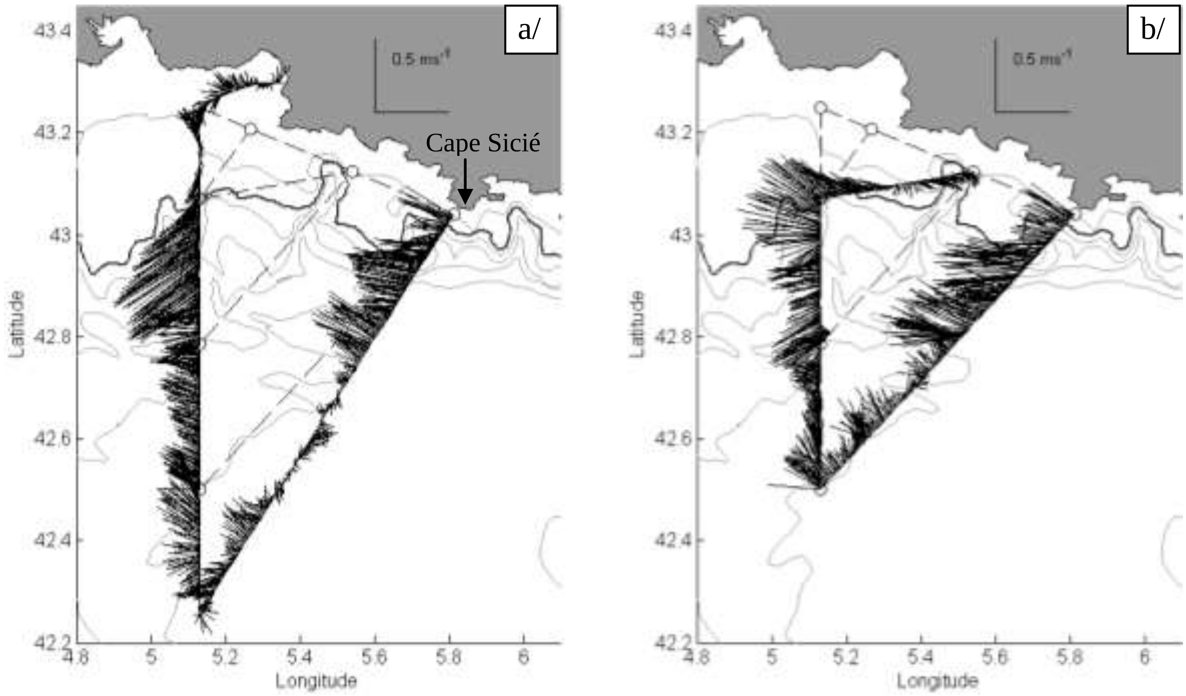

Figure 8: ADCP currents measured a/ at 24 m on 11 December 2004; b/ at 16m on 12 December 2004. Isobaths at 100, 200 (bold), 500, 1000, 1500 and 2000 m are drawn.

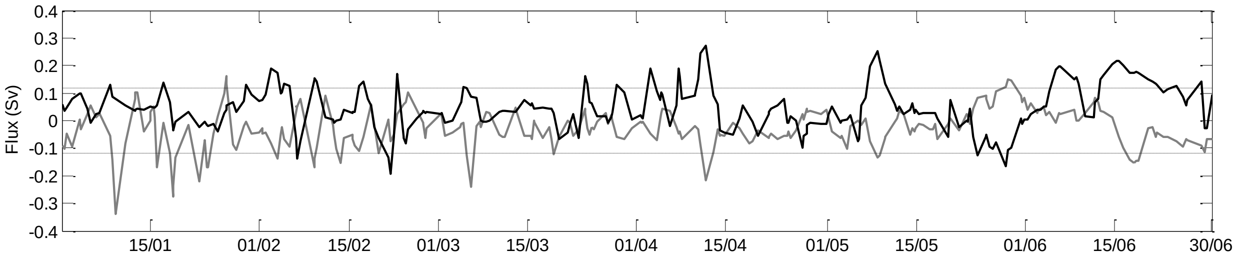

Figure 9 : Time variation over the first 6 simulated months of 2002 of west (gray) and east (black) fluxes calculated through the 200 m-deep isobath (figure 2); intrusions on the GoL are positive fluxes. Dashed lines at +/- 0.12 Sv are plotted for the analysis of extreme events.

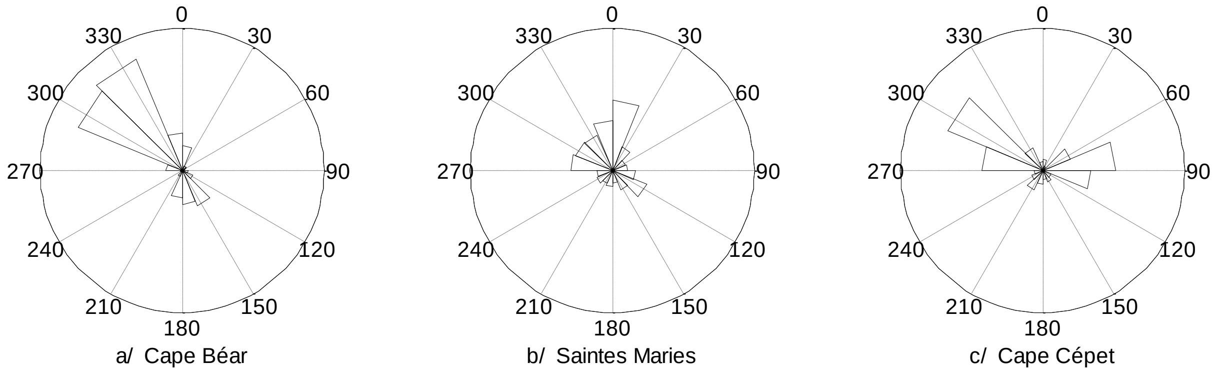

Figure 10 : Rose representation of the wind data measured at three Météo-France stations along the GoL's coastline (from January 2000 to June 2005) : a/ Cape Béar (west gulf), b/ Saintes-Maries-de-la-mer (center gulf), c/ Cape Cépet (east gulf). Angles are separated in 16 classes of 22.5°.

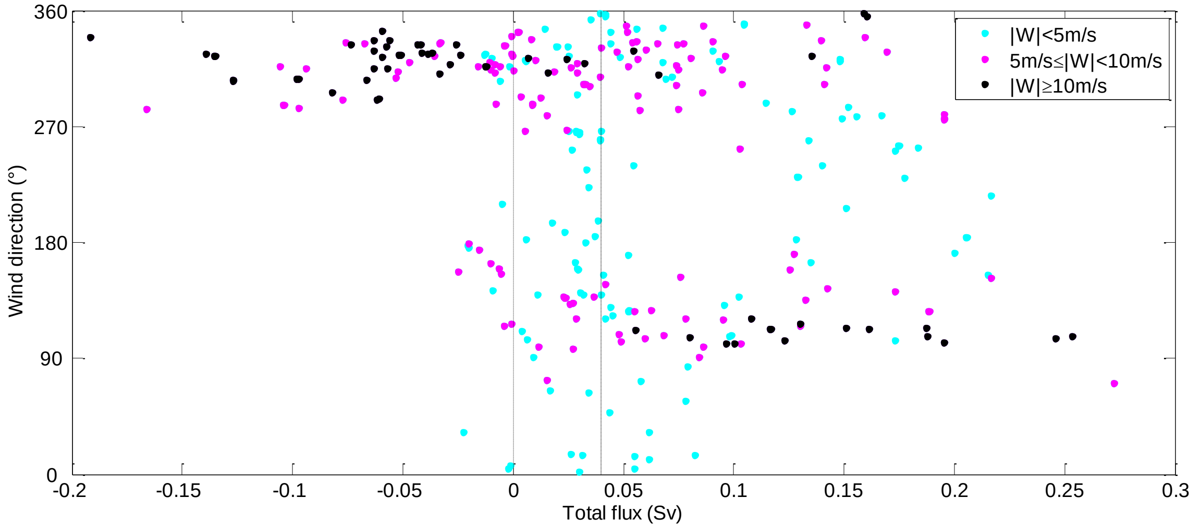

<u>Figure 11</u> : Modeled wind direction at the GOLTS mooring (5.13°E ; 43.07°N) over the first 6 months of 2002, as a function of the modeled total currents' flux on the eastern part of the GoL. The dashed line is the limit of detection of intrusions (fluxes > 0.04 Sv). The three color categories are function of wind intensity.

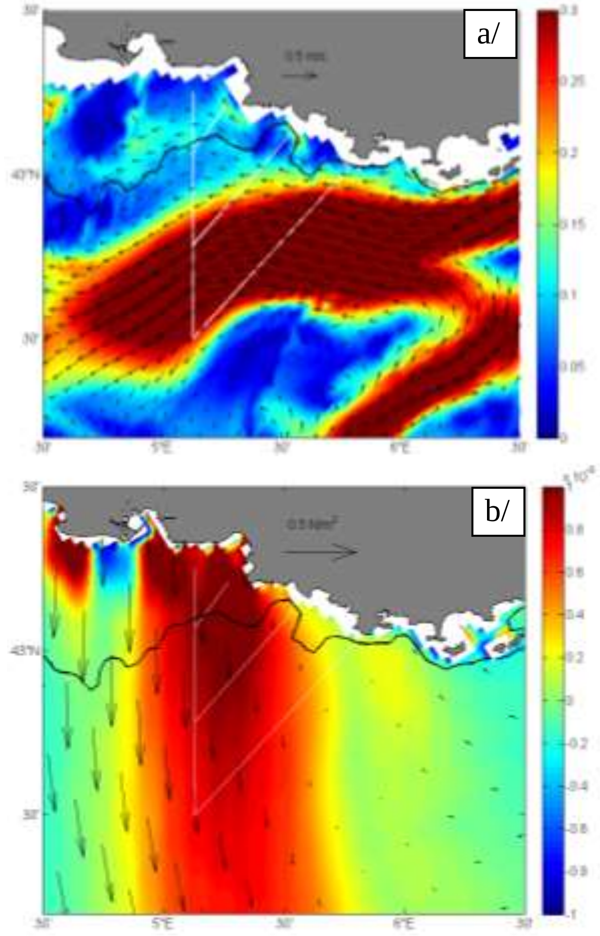

Figure 12 : a/ currents (arrows and color) simulated at 48 m on 24 March 2002, b/ wind stress curl (in color, N/m^3) and wind stress (in arrows, N/m^2) throughout the GoL. Isobath 200 m is the black bold line. GOLTS transects are in white.

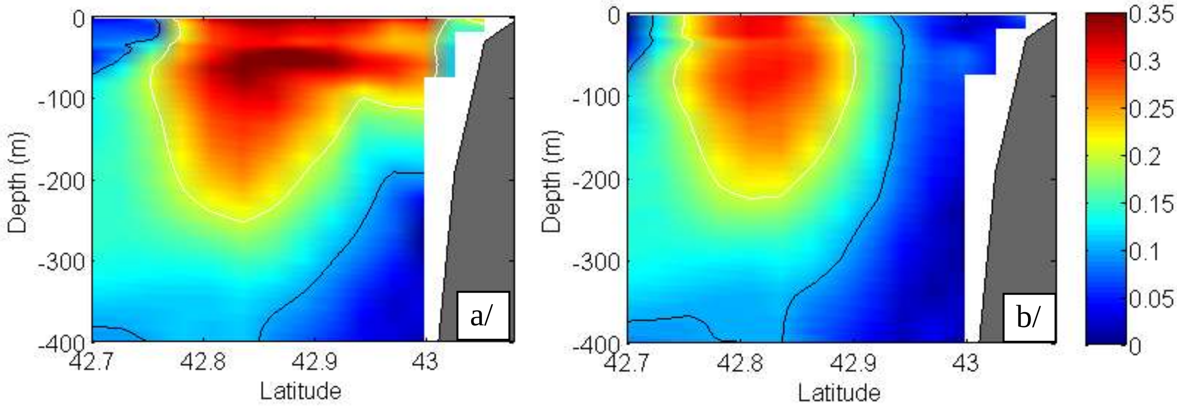

Figure 13: Vertical sections of the simulated currents' intensity (m/s) at longitude 5.85°E off the Cape Sicié on 8 May 2002 a/ in the 3 km simulation and b/ in the 3 km simulation without east wind. Isotachs at 0.20 m/s and 0.10 m/s are respectively drawn in white and in black.

TABLES

Table 1: Current fluxes[1] calculated through the 12 GOLTS cruises. The symbol Ø indicates no intrusion was detected.

GOLTS cruises		NC's flux (Sv)[2]	Intrusions' flux (Sv)
2002	June	0.70 - 1.15 - 1.02 - 1.26	0.07 - 0.09 - 0.11 - 0.05
	October	0.77*	0.15 - 0.22
	December	1.01 - 2.25	0.32 - 0.16 - 0.15
2003	March	1.32	0.13
	June	1.13	0.04
	December	1.15* - 1.47*	0.17* - Ø - 0.12 - 0.37*
2004	March	1.09*	0.05
	April	0.82 - 0.73	0.08
	June	Not possible[3]	Not possible[3]
	September	0.89* - 0.73*	Ø
	December	1* - 1.21*	0.32 - 0.34 - 0.36* - 0.14 - 0.08 - 0.20 - 0.08* - 0.13
2005	April	1.29 - 0.59*	0.10 - 0.14 - 0.11

* underestimated fluxes due to a loss of range of the hull-mounted ADCP,

[1] NC's flux and intrusion flux are not calculated on the same transects hence there is not strictly temporal correspondence between the two columns. Nonetheless, all cruises take place in 1 to 5 days,

[2] NC's flux: only flux calculated through transects 6 to 7 (figure 1),

[3] ADCP depth range was not good enough to calculate fluxes.

Table 2: main modeling characteristics

SYMPHONIE model	References
Conservation equation for T, S	*Marsaleix et al.*, 2008
Advective scheme	*Beckers*, 1995
Turbulent scheme	*Gaspar et al.*, 1990
Time splitting mode	*Blumberg and Mellor*, 1987
Hybrid vertical coordinate	*Ulses et al.*, 2008a
Temporal discretisation	leapfrog scheme + *Asselin* [1972] filter
OBC	*Marsaleix et al.*, 2006
Air-sea fluxes : bulk formulae	*Geernaert*, 1990; *Estournel et al.*, 2009
Meteorological forcing	ALADIN, Météo-France
River runoff	*Estournel et al.*, 2001, 2009